The Effects of Mismatch between SPECT and CT Images on Quantitative Activity Estimation – A Simulation Study

Yingqing Lyu
University of Macau
Yue Chen
Southwest Medical University
Greta Mok (gretamok@um.edu.mo)
University of Macau https://orcid.org/0000-0002-2962-2087

Original research

Keywords: misregistration, targeted radionuclide therapy, SPECT/CT, attenuation correction, segmentation

Posted Date: June 22nd, 2021

DOI: https://doi.org/10.21203/rs.3.rs-619011/v1

The Effects of Mismatch between SPECT and CT Images on Quantitative Activity Estimation – A Simulation Study

Yingqing Lyu[1], Yue Chen[2] and Greta S. P. Mok[1, 3 *]

[1] Biomedical Imaging Laboratory (BIG), Department of Electrical and Computer Engineering, Faculty of Science and Technology, University of Macau, Taipa, Macau SAR, China

[2] Department of Nuclear Medicine, The Affiliated Hospital of Southwest Medical University; Nuclear Medicine and Molecular Imaging Key Laboratory of Sichuan Province, Luzhou, Sichuan, China

[3] Center for Cognitive and Brain Sciences, Institute of Collaborative Innovation, University of Macau, Taipa, Macau SAR, China

* Correspondence: gretamok@um.edu.mo.

Background: Quantitative activity estimation is essential in targeted radionuclide therapy dosimetry. Misregistration between SPECT and CT images at the same imaging time point due to patient movement degrades accuracy. This work aims to study the mismatch effects between CT and SPECT data on attenuation correction (AC), volume-of-interest (VOI) delineation and registration for activity estimation.

Methods: Nine 4D XCAT phantoms were generated at 1, 24, and 144 hrs post In-111 Zevalin injection, varying in activity distributions, body and organ sizes. Realistic noisy SPECT projections were generated by an analytical projection and reconstructed with quantitative OS-EM method. CT images were shifted from -5 to 5 voxels as well as according to clinical reference corresponding to SPECT images at each time point. For AC effect, mismatched CT images were used for AC in SPECT reconstruction while VOIs were mapped out from matched CTs. For VOI effect, target organs were mapped out using mismatched CTs with matched CTs for AC. For registration effect, non-rigid registrations were performed on sequential mismatched CTs to align corresponding SPECT images, with no AC and VOI mismatch. Bi-exponential curve fitting was performed to obtain time-integrated activity (TIA). Organ activity errors (%OAE) and TIA errors (%TIAE) were calculated.

Results: According to clinical reference, %OAE was larger for organs near ribs for AC effect, e.g., -2.58%±0.81% for liver. For VOI effect, %OAE was larger for small and low uptake organs, e.g., -11.94%±10.34% for spleen. %OAE was proportional to mismatch magnitude, e.g., 4.77%±1.41%, 12.01%±3.97% and 42.81%±6.38% for 1-, 2-, and 5-voxel mismatch for lungs. For registration effect, %TIAE were larger when mismatch existed in more numbers of SPECT/CT images, while no substantial difference was observed when using mismatched CT at different time points for registration reference. %TIAE was highest for VOI, followed by registration and AC, e.g., 37.61%±5.08%, 14.25%±7.07% and 1.13%±0.90% respectively for kidneys.

Conclusions: The mismatch between CT and SPECT images poses a significant impact on accuracy of quantitative activity estimation in dosimetry, attributed particularly from VOI delineation errors. It is recommended to perform registration between emission and transmission images at the same time point to ensure dosimetric accuracy.

Keywords: misregistration, targeted radionuclide therapy, SPECT/CT, attenuation correction, segmentation.

1. Introduction

Targeted radionuclide therapy (TRT) is an effective therapy for various types of cancers [1], using radionuclides labeled molecules to kill cancer cells with ionizing radiation by destroying their DNA in the cell nucleus and by “bystander” effects [2], resulting in tumor shrinkage. Compared to conventional chemotherapy, TRT aims to specifically deliver a lethal dose targeting cancerous cells with minimal collateral toxicity to the surrounding normal organs or tissues, which requires accurate drug biodistribution information prior and post treatment. Such information can be obtained by planar imaging or emission computed tomography, i.e., SPECT and PET [3]. Sequential quantitative activity images at different time points or sometimes single time point for Y-90 radioembolization allow the estimation of time-integrated activity (TIA) for critical organs and tumors by fitting of time-activity curves (TACs) and obtain the area under the curves for further dose conversion.

Integrated CT in SPECT/CT can be used for attenuation correction (AC) in SPECT reconstruction to improve quantitative accuracy, and provide anatomical reference for the activity uptakes in general. For TRT dosimetry, CT data can be further used in segmentations of tumors and critical organs, or registrations to reduce the misalignments among serial scans [4, 5]. However, the accuracy of registration between SPECT and CT data is limited by certain voluntary and involuntary motion since CT scans take couple seconds while SPECT imaging needs at least several minutes. Voluntary variables are mainly due to patient movement between SPECT and CT scans as the patient position may change during the two acquisitions. Involuntary movements are mostly physiological activities, such as the beating of the heart, the peristalsis of the bowel [6] and the respiratory movements of the lungs and adjacent organs [7]. Respirations cause organ movement or deformation particularly in the upper abdominal [8] and lower thoracic regions [9, 10]. The SPECT and CT mismatch may manifest as patients may practice breath holding during CT scans, while SPECT images are acquired during free breathing, leading to data at different respiratory positions being acquired. Such movements alter the appearance of organ shape, size, and location between the SPECT and CT imaging sessions, being responsible for the minor mismatches. Voluntary and involuntary mismatch errors not only cause artifacts in the SPECT data due to the use of misaligned CT for AC [11, 12], but also misleading anatomical localization for later segmentation required for dosimetric calculations. He et al. have studied the impact of SPECT/planar and CT misregistration at the same imaging time point and mis-definition of volume-of-interest (VOI) from manual segmentation on activity estimation [13]. In their study, VOI misregistration errors were generally larger than mis-definition errors, producing a considerable source of errors on activity estimations. For planar images, the quantitation error could be up to 8% for the kidneys with only 1 voxel VOI mismatch in z-direction between planar and CT images. Although SPECT images were less sensitive to the VOI misregistration errors than the planar images, the error was about -5% for the spleen if SPECT and CT images had 1 voxel VOI mismatch in y-direction. One limitation of their study is that only mismatch within 1 voxel, i.e., 4.42 mm, between SPECT and CT is evaluated, whereas the mean misregistration for integrated SPECT/CT at the same time point could reach 10.2±4.3 mm for 3 directions, with a range of 0-25.1 mm [14].

Besides, for serial imaging sessions, CT images are usually used for registration and the resultant motion field will be used to align the corresponding SPECT images to reduce the misalignments at different time points [15]. Thus, a mismatch of SPECT and CT at the same time point would lead to TIA estimation errors when using CT images for registration reference. All the aforementioned errors will propagate to final TIA estimation, and are expected to accumulate for more number of imaging time points.

This study aims to systematically evaluate the impact of mismatch between CT and SPECT images in the following aspects using simulations: (i) AC; (ii) VOI definition; and (iii) registration among sequential SPECT/CT images.

2. Materials and Methods

2.A. Phantom Population

A population of nine 4D digital extended cardiac torso (XCAT) phantoms was used [16]. The XCAT phantoms with highly detailed body anatomies and physiological functions were generated using non-uniform rational B-spline (NURBS) and subdivision surfaces based on segmentation of patient datasets. It is an important imaging tool that allows modeling with user-defined parameters, i.e., anatomical variations, cardiac and respiratory motion, generating realistic multimodal imaging data close to the clinical studies. The phantoms used in this study varied in three anatomical variations with three respective In-111 Zevalin activity distributions (Figure 1), modeling an axial respiratory motion of 20 mm and 5 s period as well as normal cardiac motion. The activity distribution in the background remainder, kidneys, spleen, liver, heart, bone marrow and blood vessel was uniform except for the lungs since there was no airways activity. The time-varying activity and effective half-life of each organ were based on a set of clinical patient data [17] to simulate whole body SPECT scans covering from the thorax to the abdomen at 3 time points, i.e., 1, 24, and 144 hrs post-injection.

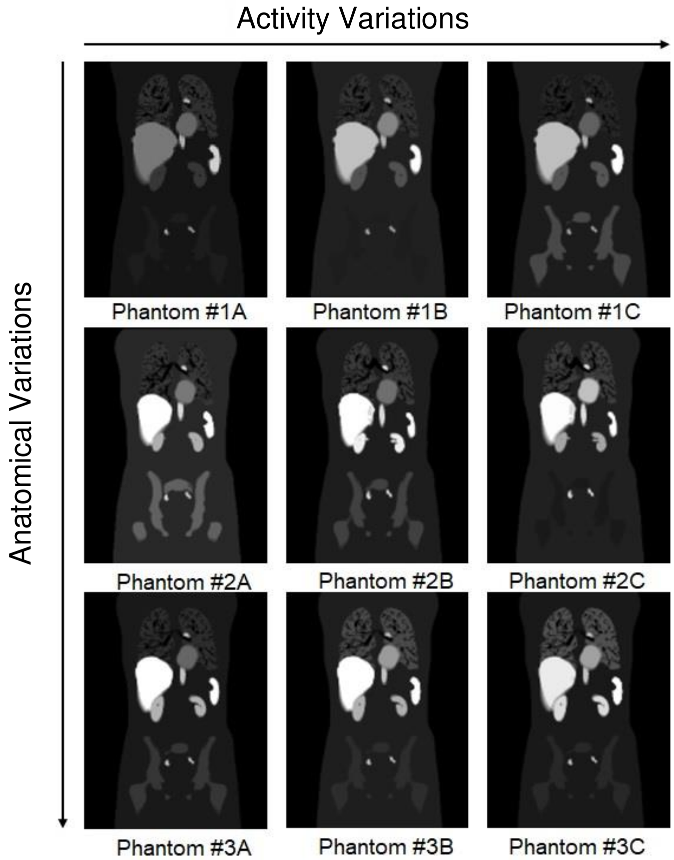

Figure 1: Sample activity maps of the 9 XCAT phantoms.

2.B. Simulation and Quantitative Reconstruction

An analytical projector of a medium energy general purpose (MEGP) collimator modeling attenuation, scatter, and geometric collimator-detector-response (GCDR) was used [18] for the simulations based on a GE Discovery VH Hawkeye SPECT/CT system with crystal thickness of 2.54 cm. Considering two photopeaks of In-111, i.e., 171 keV and 245 keV with abundances of 90.2% and 94% respectively, the attenuation maps with abundance weighted average energy of 210 keV for AC in reconstruction were generated [19]. The scatter was modeled by the effective source scatter estimation (ESSE) method [20] and the GCDR was performed using an analytic formulation proposed by Metz et al [21].

The noise-free projections were generated in 128 transaxial and 170 axial bins with 4.42 mm voxel size and 128 views over 360° acquisition, using phantoms with a voxel size of 2.21 mm. A system calibration factor of 1.43×10^{-4} counts $s^{-1}Bq^{-1}$ was used to scale the projections to a clinical count level of 30 s/view acquisition time, which were then added with Poisson noise to obtain realistic noisy projections. The data were reconstructed using the OS-EM algorithm (8 iterations and 16 subsets, i.e., 128 updates) with attenuation, ESSE and GCDR compensation.

2.C. Experimental Design

2.C.1. The Mismatched AC Effect

The SPECT/CT mismatch effect on AC was evaluated on 1 time point for organ activity and 3-time point for TIA estimation, respectively.

2.C.1.a. Organ activity estimation

SPECT and its corresponding CT images at 24 hr time point for 9 phantoms were used for analysis. The CT image was first shifted from 0 to 5 voxels (0-22.1 mm) in anterior-to-posterior (y-), superior-to-inferior (z-) and lateral (x-) directions respectively as compared to the corresponding SPECT image. The increments were 0.1 voxel for 0 to 1 voxel, 0.2 voxel for 1 to 2 voxels and 1 voxel for 2 to 5 voxels respectively. We also evaluated the random mismatch between CT and SPECT images where CT images were shifted randomly within the mean Euclidian distance of 10.2±4.3 mm (2.31±0.97 voxels) and a maximum range of 25.1 mm (5.67 voxels) as compared to the corresponding SPECT images according to a clinical reference [14]. The noisy projections were reconstructed using the mismatched CT maps for AC (Figure 2). VOIs of the target organs, i.e., kidneys, spleen, liver and lungs were segmented from the matched CT images semi-automatically using an open-source software application ITK-SNAP [22] to map out the corresponding organs from the SPECT images to measure the organ activities.

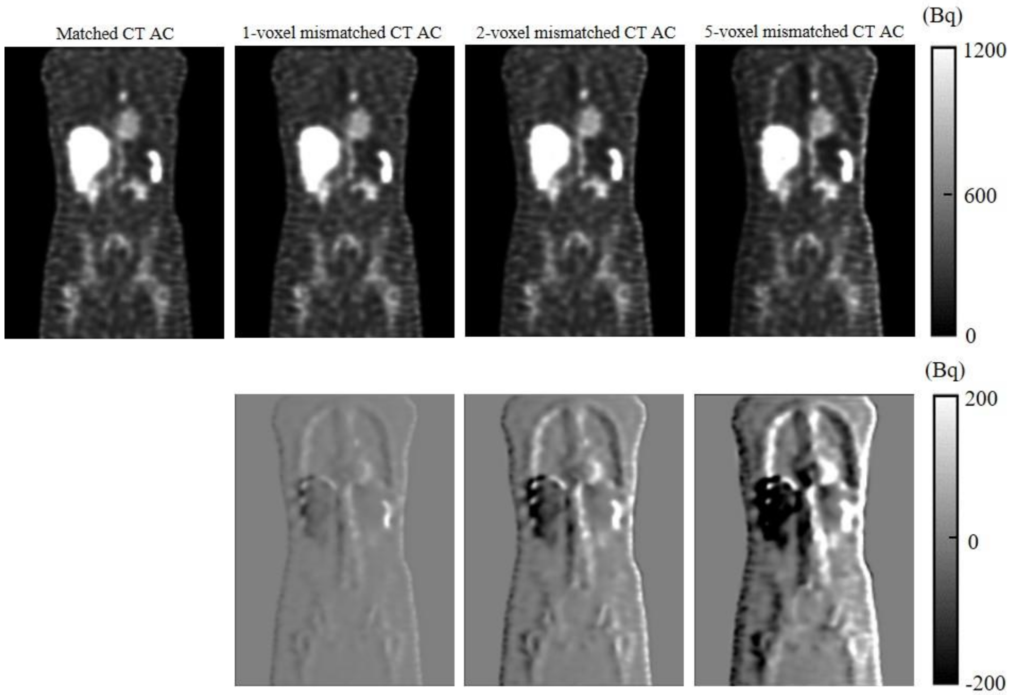

Figure 2: Top: Sample SPECT images using different CT maps for AC; Bottom: Difference images as compared to the SPECT images using matched CT for AC.

2.C.1.b. TIA estimation

SPECT and CT images at 1, 24, and 144 hr time points for 9 phantoms were used for evaluations, while misalignments were not modelled among images at different time points. CT images at 3 time points were shifted randomly within the mean and maximal range of 2.31 voxels and 5.67 voxels respectively as compared to the corresponding SPECT images, which were then used for AC for the corresponding SPECT reconstructions (Figure 3). Voxel-based bi-exponential curve fitting using the nonlinear least squares method under MATLAB 9.6 (The MathWorks Inc., Natick, USA) was performed on the sequential quantitative SPECT images over 3 time points to obtain the TIA images, i.e., area under the curves by integration. VOIs segmented from the matched CT images were used to map out the target organs from the TIA images.

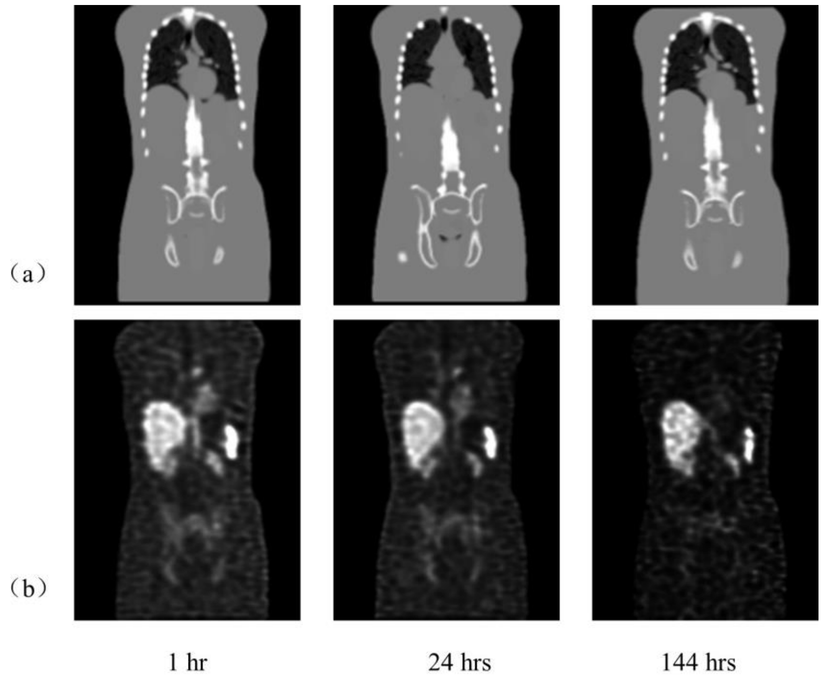

Figure 3: The mismatched AC effect for TIA estimation: (a) mismatched CT images and (b) the corresponding SPECT images at 3 different time points.

2.C.2. The Mismatched VOI Delineation Effect

Similar to the previous section, the mismatch effect on VOI delineation was investigated on organ activity and TIA estimation errors.

2.C.2.a. Organ activity estimation

The simulated noisy SPECT projections at 24-hr time point were reconstructed using the matched CT maps for AC. Then the target organs on SPECT images were mapped out using mismatched VOIs obtained from the shifted CT, generated as described in Section 2.C.1.a, to obtain the organ activities.

2.C.2.b. TIA estimation

The simulated noisy projections at 3 time points were reconstructed with corresponding matched CT maps for AC. Misalignments were not modeled among different time points. Considering the VOIs may apply on the sequential SPECT images or the TIA image directly, VOI mismatch was modeled in 1 and 3 time points respectively. For the 3-time-point VOI mismatch, target organs were mapped out from the SPECT image at each time point using the mismatched VOIs from shifted CT images as described in Section 2.C.1.b. Curve fitting and integration were then performed as described in the previous section on the segmented target organs to obtain their TIA. For the 1-time-point VOI mismatch, curve fitting and integration were first performed on the sequential SPECT images to obtain the TIA images. The target organs were then mapped out using mismatched VOI at 24-hr time point from the TIA images.

2.C.3. The Mismatched Registration Effect

To model the misalignment among sequential scans, the local organ deformation was performed for kidneys, spleen, liver, and stomach at 1 and 144 hrs time point, translated and rotated randomly within ±5 pixels (11.05 mm) or degrees, while using the 24 hrs time point as the reference. The volume change was held within 5% for each organ except the stomach. The boundaries of the lungs were defined by the deformation of surrounding organs, i.e., liver and heart. Besides the local organ deformation, to simulate the whole body movement between scans, a rigid transformation within ±5 pixels or degrees of translation or rotation was also modeled [23, 24].

2.C.3.a. Accumulative mismatched effect

Sequential CT images of the 9 phantoms were shifted randomly as compared to their corresponding SPECT images for 1-, 2- and 3-time points respectively as described in 2.C.1.b. CT images were then non-rigidly registered to the "reference image", i.e., 24-hr CT images, using the affine plus B-spline framework under the open-source program "Elastix" [25]. The resultant motion vectors were then applied to align the corresponding SPECT images with matched CT AC. The TIA images were derived by curve fitting and integration of the SPECT images over 3 time points, using the same method as described in the previous sections. VOIs segmented from the matched CT images at the 24-hr time point were used to map out the target organs from the TIA images.

2.C.3.b. Mismatch on reference images

Sequential CT images of the 9 phantoms were shifted randomly as compared to their corresponding SPECT images on 1, 24 or 144 hr-time point separately. The shifted CT images at 3 different time points were used as "reference image" respectively for registrations. The resultant motion fields were used to align the corresponding SPECT images with matched CT AC. The effect of using different time point CT images as registration reference was also evaluated for sequential SPECT/CT images with no SPECT and CT mismatch for comparison. Curve fitting and integration were performed on the "registered" images to obtain the TIA images, and TIAs for target organs were then mapped out using matched VOIs at the reference time point.

2.D. Data Analysis

For the errors in organ activity estimation introduced by mismatched SPECT and CT images at 1 time point caused by AC and VOI delineation, the target organ activities ($\boldsymbol{A_{w/mismatch}}$) were compared to the reference ($\boldsymbol{A_{ref}}$), i.e., organ activities obtained with no misalignment between SPECT and CT images to calculate the organ activity errors (%OAE):

$$\boldsymbol{\%OAE = \frac{A_{w/mismatch} - A_{ref}}{A_{ref}} \times 100\%} \quad \textbf{(1)}$$

Positive values indicate overestimation and negative values indicate underestimation of the organ activity.

For the errors in TIA estimation caused by sequential mismatched SPECT and CT images, the absolute TIA error (%TIAE) for the target organs ($\boldsymbol{TIA_{w/mismatch}}$) was defined as the following equation, using sequential SPECT and CT images with no SPECT/CT mismatch and no misalignment between different time points for registration as reference ($\boldsymbol{TIA_{ref}}$):

$$\%\boldsymbol{TIAE} = \frac{|\boldsymbol{TIA_{w/mismatch}} - \boldsymbol{TIA_{ref}}|}{\boldsymbol{TIA_{ref}}} \times \mathbf{100}\% \qquad \textbf{(2)}$$

The %TIAE obtained from Section 2.C.1.b, 2.C.2.b and 3-time-point mismatch for registration in 2.C.3.a were compared to demonstrate the error magnitudes from AC, VOI delineation and registration for TIA measurement caused by SPECT and CT mismatch. Statistical analysis was performed using the paired t-test with Bonferonni correction by SPSS Version 24 (IBM Corp., Armonk, NY, USA) for %TIAE. A p value < 0.05 was defined as significantly different.

3. Results

3.A. The Mismatched AC Effect

Figure 4 shows the %OAE for target organs by the mismatched AC effect for Phantom #2A. The %OAE for the mismatch between SPECT and CT images along x- and z-directions were larger than y-direction for all target organs especially for spleen, liver and lungs, e.g., %OAE for spleen at 5 voxels were -17.04%, 3.81% and -19.55% for x-, y-, z-direction respectively. The mismatch of attenuation maps had larger errors for organs near ribs, e.g., spleen and lungs. The %OAE results of 9 phantoms were consistent (Table 1). The errors are generally <3% for mismatch according to the clinical reference.

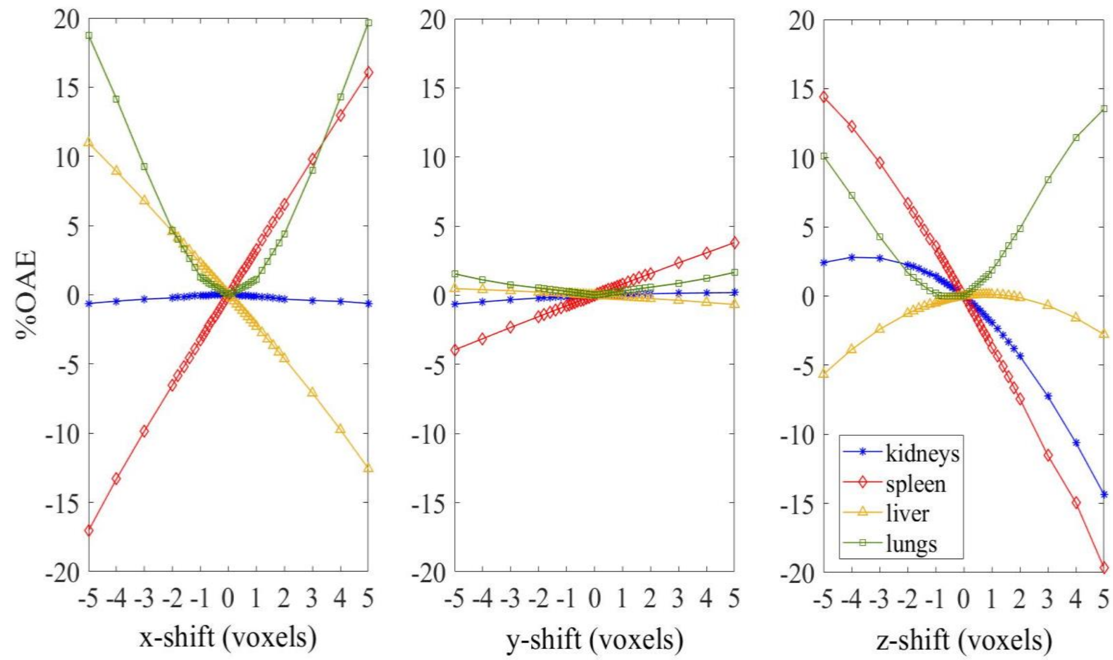

Figure 4: %OAE introduced by shifting CT images from -5 to 5 voxels for the AC effects. Left: x-direction; middle: y-direction; right: z-direction.

Table 1: Mean %OAE and standard deviation of 9 phantoms for the mismatched AC effect.

		kidneys	spleen	liver	lungs
x-shift	-1 voxel	-0.11%±0.06%	-4.01%±0.35%	2.73%±0.20%	1.17%±0.18%
	-2 voxels	-0.32%±0.12%	-8.00%±0.71%	5.46%±0.41%	4.25%±0.56%
	-5 voxels	-1.61%±1.25%	-20.20%±1.60%	13.43%±1.10%	17.30%±2.40%
y-shift	-1 voxel	-0.20%±0.07%	-0.37%±0.19%	0.20%±0.04%	0.19%±0.10%
	-2 voxels	-0.40%±0.13%	-0.83%±0.33%	0.31%±0.08%	1.06%±0.49%
	-5 voxels	-0.96%±0.25%	-2.28%±0.76%	0.55%±0.19%	4.38%±2.29%
z-shift	-1 voxel	1.54%±0.35%	3.43%±0.17%	-0.20%±0.15%	0.41%±0.09%
	-2 voxels	2.30%±0.58%	5.62%±0.54%	-0.62%±0.30%	1.67%±0.14%
	-5 voxels	3.03%±1.21%	11.84%±1.38%	-3.90%±0.84%	9.86%±1.35%
Mismatch according to clinical reference		**-0.72%±0.50%**	**2.13%±1.34%**	**-2.58%±0.81%**	**1.54%±0.28%**

3.B. The Mismatched VOI Delineation Effect

Figure 5 shows the %OAE for the mismatched VOI delineation effects for Phantom #2A. The %OAE for VOI effect was larger on small organs, i.e., kidneys and spleen, and organs with lower activity uptake, e.g., lungs. The results show that the mismatch errors were proportional to the magnitude of the CT mismatches. The %OAE results of 9 phantoms were consistent (Table 2). The errors could reach >10% for spleen for mismatch according to the clinical reference.

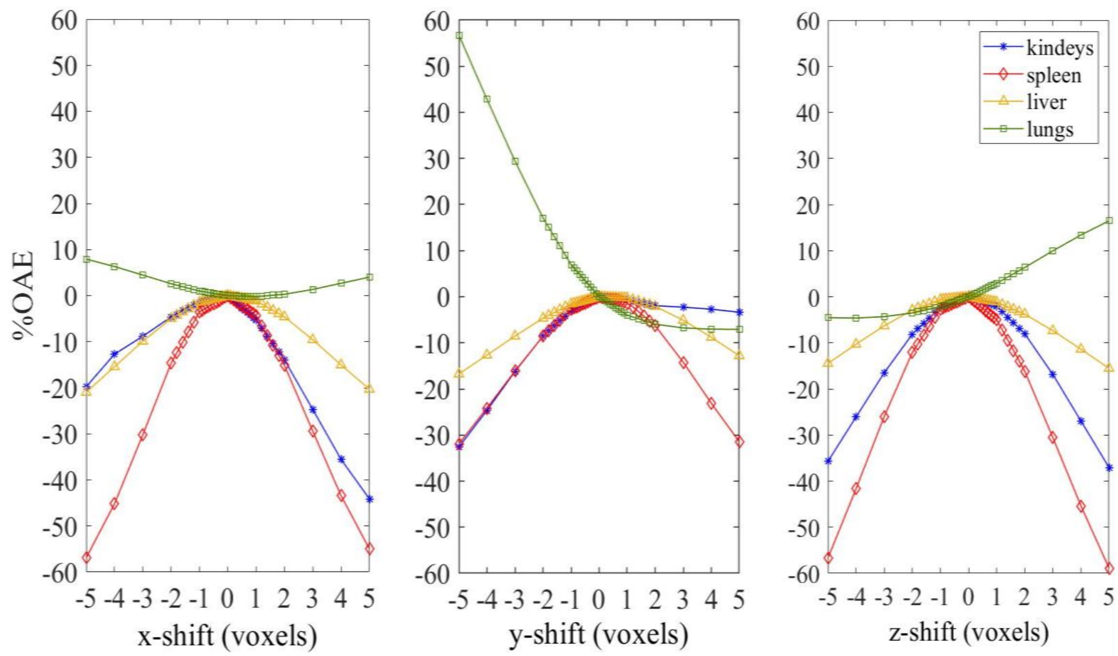

Figure 5: %OAE introduced by shifting CT images from -5 to 5 voxels for the mismatched VOI delineation effects. Left: x-direction; middle: y-direction; right: z-direction.

Table 2: Mean %OAE and standard deviation of 9 phantoms for mismatched VOI delineation effect.

		kidneys	spleen	liver	lungs
x-shift	-1 voxel	-1.08%±1.24%	-2.22%±0.92%	-1.47%±0.24%	0.59%±0.31%
	-2 voxels	-3.17%±1.65%	-10.02%±3.00%	-4.86%±0.54%	1.42%±0.93%
	-5 voxels	-16.37%±3.24%	-42.83%±7.94%	-19.79%±2.01%	4.82%±3.07%
y-shift	-1 voxel	-4.07%±1.16%	-1.81%±0.94%	-1.21%±0.37%	4.77%±1.41%
	-2 voxels	-9.58%±1.86%	-6.43%±1.80%	-3.88%±0.83%	12.01%±3.97%
	-5 voxels	-30.97%±4.14%	-26.43%±3.57%	-14.98%±2.07%	42.81%±6.38%
z-shift	-1 voxel	-1.94%±0.45%	-3.65%±1.00%	-0.84%±0.23%	-1.86%±0.47%
	-2 voxels	-7.15%±1.71%	-13.64%±2.69%	-3.11%±0.45%	-3.25%±1.24%
	-5 voxels	-32.46%±8.03%	-55.93%±6.58%	-13.83%±1.06%	-6.00%±3.94%
Mismatch according to clinical reference		**-9.14%±8.47%**	**-11.94%±10.34%**	**-4.38%±2.88%**	**5.97%±4.36%**

3.C. The Mismatched Registration Effect

Figure 6 shows the %TIAE results for different numbers of SPECT and CT mismatch existed in a 3-time point study. For sequential imaging sessions, errors increased when the frequency of mismatches between SPECT and CT images increased, e.g., %TIAE for kidneys was 6.47%±4.68%, 9.60%±5.14%, and 14.25%±7.07% respectively for 1-, 2-, and 3-time point SPECT/CT mismatches. Significant differences were observed between mismatch at 1 and 3 time points for all target organs.

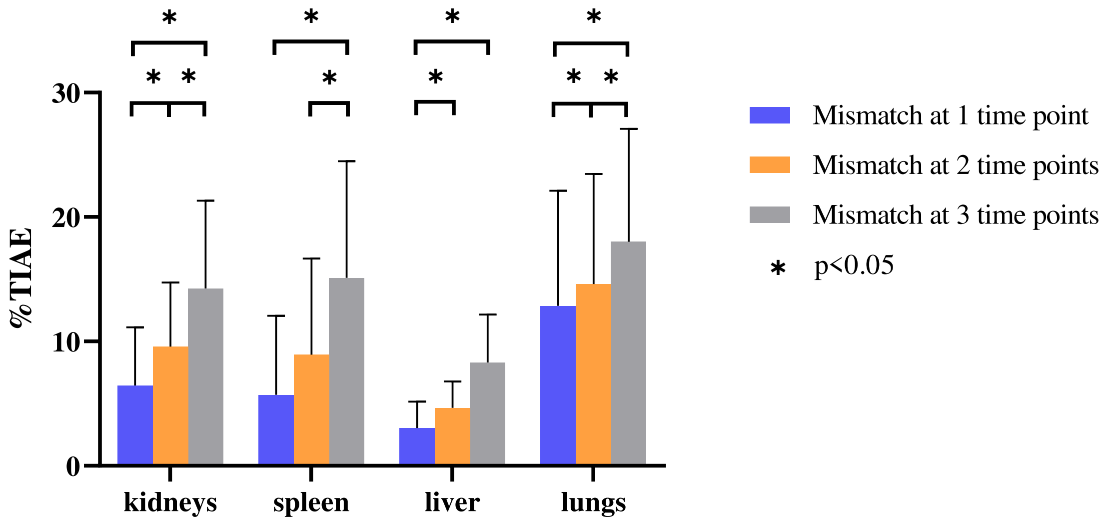

Figure 6: %TIAE for target organs with 1-, 2-, and 3-time-points SPECT/CT mismatch. All results represent the average of 9 phantoms and error bars show the standard deviation.

Figure 7 shows the results of using the different time point CT as "reference image" for registration for sequential CT images to then register the corresponding SPECT images. There was no statistically significant difference among %TIAE for the CT reference at different time points, no matter when using mismatched or matched CT as registration reference. The %TIAE was generally larger for the mismatched CT registration (Figure 7a) as compared to matched CT registration (Figure 7b). The %TIAE was smaller when mismatch occurs at 1- or 24-hr as compared to 144-hr time point as the registration reference in this study (Figure 7a).

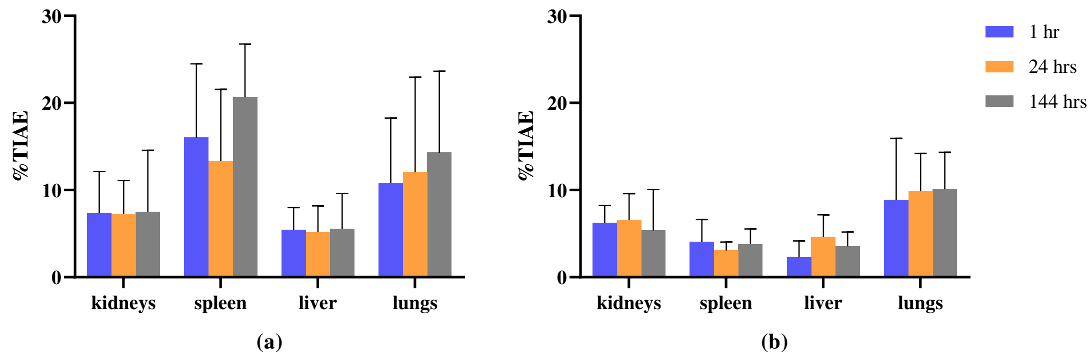

Figure 7: %TIAE for target organs when using (a) mismatched and (b) matched CT image at different time points as registration reference. All results represent the average of 9 phantoms and error bars show the standard deviation.

Figure 8 compares the %TIAE results for SPECT and CT mismatch for AC, VOI and registration effects. The %TIAE for the AC effect was the smallest while the VOI effect for the 3-time-point mismatch was the largest for all organs, e.g., 1.13%±0.90%, 37.61%±5.08% and 14.25%±7.07% respectively for mismatched AC, VOI (3-time-point mismatch) and registration effects for kidneys. Even for VOI mismatch occurred in 1-time point, i.e., target organs mapped out 1 time using mismatched VOI from the TIA images, its %TIAE was still generally larger than 3-time point AC and registration mismatch effects for most organs except for the lungs, where registration mismatch affected more on their TIA estimation. In addition, the %TIAE for the 3-time-point mismatched VOIs effect was larger as compared to the 1-time-point mismatched VOIs for all organs as expected, e.g., %TIAE for spleen was 44.86%±4.60%, 22.94%±10.29% for the 3- and 1-time point VOI mismatch respectively. Significant differences were observed among different effects except for the registration and 1-time-point VOI mismatch effect.

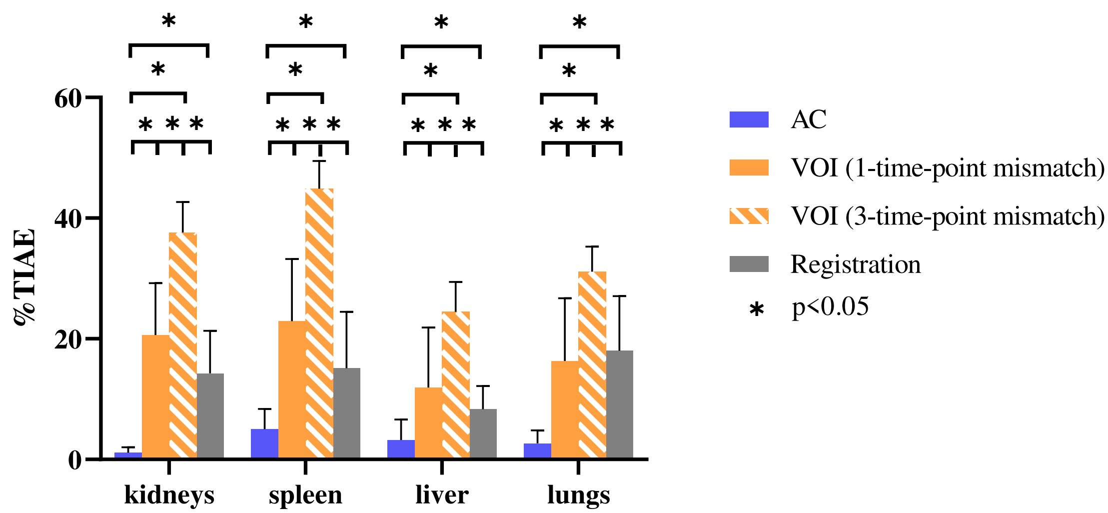

Figure 8: %TIAE for different target organs with the AC, VOI and registration mismatch effects. All results represent the average of 9 phantoms and error bars show the standard deviation**.**

4. Discussion

In this work, the errors of mismatches caused by patient movement between CT and SPECT scans at the same time point were evaluated systematically, including the %OAE for AC and VOI effects at one scanning time point and the %TIAE from sequential images taken at different time points. All results showed that the mismatches between CT and SPECT images influence activity estimation and will further affect the TIA estimation. Goetze et al. [14] demonstrated the misregistration frequently occurred between SPECT and CT images in myocardial perfusion SPECT/CT, i.e., about two thirds of the clinical cases showed more than one voxel of misregistration. They demonstrated that the mean misregistration was 10.2±4.3 mm, with a range of 0–25.1 mm. Thus, besides fixed range of mismatch, CT images in this study were shifted as compared to the SPECT images within the mean and maximal range (2.31 voxels, i.e., 10.2 mm and 5.67 voxels, i.e., 25.1 mm respectively) according to their study.

The %OAE results revealed the trends and magnitude of errors in activity estimates resulting from AC and VOI effects. The AC errors of the organs near ribs showed a larger impact compared with the organs far from the ribs. This could be attributed to the larger attenuation coefficient of bone as compared to the soft tissues. For instance, when the CT maps is shifted to the right, the ribs could be moved into the liver region and would cause over attenuation compensation thus activity overestimation in the liver. On the contrary, if the CT is shifted to the left, the background could move into the liver, leading to the underestimation of the liver activity. Moreover, the ribs movement is not much in the y-direction as compared to other directions, thus the %OAE is relatively smaller for the AC mismatch effect in this direction.

For VOI mismatch effect, %OAE was larger for small organs, such as kidneys and spleen, and low uptake organs that are close to the high uptake organs, e.g., the lungs. For example, for VOI mismatch according to clinical reference, the %OAE can reach -11.94%±10.34% for the spleen. All target organs except the lungs showed activity underestimation since the adjacent region had lower activities. Overestimation was expected for the lungs, since they were near to the heart and liver with higher activity. These results were in accordance with the results from another study [13].

For registration mismatch effect, we evaluated the errors for using mismatched CT images at different time points as the “reference image” and different numbers of mismatch occurred in sequential SPECT/CT. No significant difference was observed when using different time point images for registration reference, probably attributed to the fact that CTs at different imaging points possess similar image intensity while it is different in sequential SPECT images for SPECT-based registration [5]. For a 3-time point imaging study, %TIAE is >10% for kidneys, spleen and lungs when SPECT and CT mismatch accumulates for 3 SPECT/CT sessions (Figure 6).

The VOI errors were larger than the AC errors in both organ activity and TIA estimation, especially for small organs, such as kidneys and spleen. The %ODE for kidneys and spleen were -9.14%±8.47% and -11.94%±10.34% for 1-time point SPECT and CT random VOI mismatch, which were further accumulated in TIA calculation by sequential mismatched images, i.e., the %TIAE for kidneys and spleen were 37.61%±5.08% and 44.86%±4.60% for 3-time-point mismatched VOI and 20.62%±8.61% and 22.94%±10.29% for 1-time-point mismatched VOI respectively. The VOI errors were generally largest, followed by registration and AC errors in TIA estimation.

Simulation provides an effect means for evaluation with known truth, i.e., organ activity and time integrated activity in this study. Moreover, different mismatch schemes can be modeled based on the clinical reference [14]. In this study, rigid mismatch is modelled between the SPECT and CT, which should be a legitimate assumption for voluntary motion happened between the same time point SPECT and CT due to the relatively short time gap. However, nonrigid motion deformation may exist between the same time point SPECT and CT from involuntary motion, e.g., respiratory motion, and also impact the dosimetric accuracy. For example, liver and lungs mis-registration between the mismatched SPECT/PET and CT due to respiration in Y-90 microsphere treatment planning or dose verification for primary or metastatic cancers in liver is commonly observed in the clinics, posing uncertainties for then dosimetric calculations. Associate results are published in our recent study [26]. However, registration between mismatched SPECT and CT due to respiration could be challenging due to the substantially inherent motion blur thus unclear organ boundaries from the static emission images. Respiratory gating and motion compensation could be a possible solution [27]. Although restraints and careful position could reduce patients' movement, our results indicate that non-negligible mismatches between SPECT and CT images at the same time point could affect the dosimetric accuracy >40% especially for small organs and low uptake organs (Figure 8), while the accuracy of organ activity estimation for quantitative SPECT exceeds 90% with appropriate compensation [28]. Thus, alleviating the mismatch between transmission and emission images by registration is necessary to improve the AC, VOI delineation and the then CT-based registration among serial scans for TRT dosimetry. Lesions are not simulated in this study as for the maximal tolerated dose regime, absorbed dose for critical organs are more important. However, SPECT and CT mismatch impact on lesions are expected to be similar or even more severe to small organs, i.e., spleen in this study. Although this study is based on simulations with

In-111 Zevalin distribution, results should be applicable to other common clinical applications such as Lu-177 tracers nowadays.

5. Conclusion

This work studied the mismatch effects between SPECT and CT scans at the same time point, including the activity estimation errors caused by the AC and VOI delineation, and TIA estimation errors from AC, VOI delineation and registration from sequential SPECT/CT scans. Our results showed that dosimetric estimation errors increase as the mismatch magnitude increases. It was observed that the VOI errors were the largest, followed by registration and AC errors for dosimetric estimations, especially for the small organs and low uptake organs in this study. Quantitative errors could reach 40% for SPECT and CT mismatch modeled according to a clinical reference. Registration between the same time point SPECT and CT is recommended to enhance dosimetric accuracy.

Abbreviations

SPECT/CT: Single photon emission computed tomography/computed tomography; SPECT: Single photon emission computed tomography; CT: Computed tomography; AC: Attenuation correction; VOI: Volume-of-interest; GCDR: Geometric collimator-detector-response; TIA: Time-integrated activity; OAE: Organ activity error; TIAE: Time-integrated activity error; TRT: Targeted radionuclide therapy; TAC: time-activity curve; XCAT: 4D digital extended cardiac torso; MEGP: Medium energy general purpose; ESSE: Effective source scatter estimation; OS-EM: Ordered subset expectation maximization.

Acknowledgements

Not applicable.

Authors' contributions

Yingqing Lyu and Greta Mok were both the primary writers of the manuscript. Yingqing Lyu was mainly responsible for phantom generation, data collection and analysis while Greta Mok and Yue Chen were responsible for the simulation design, data interpretation and study integration.

Funding

This work was supported by research grants from Science and Technology Development Fund of Macau (0091/2019/A2) and Natural Science Foundation of China (81922080).

Availability of data and materials

The datasets used and analyzed during the current study are available from the corresponding author on reasonable request.

Ethics approval and consent to participate

Not applicable.

Consent for publication

Not applicable.

Competing interests

The authors declare that they have no competing interests.

Reference:

1. Gudkov SV, Shilyagina NY, Vodeneev VA, Zvyagin AV. Targeted radionuclide therapy of human tumors. Int J Mol Sci. 2016;17:33. https://doi.org/10.3390/ijms17010033.
2. Kassis AI, Adelstein SJ. Radiobiologic principles in radionuclide therapy. J Nucl Med. 2005; 46 Suppl 1:4S-12S.
3. Li T, Ao ECI, Lambert B, Brans B, Vandenberghe S, Mok GSP. Quantitative Imaging for Targeted Radionuclide Therapy Dosimetry - Technical Review. Theranostics. 2017;7:4551-65. https://doi.org/10.7150/thno.19782.
4. Li T, Wu NY, Song N, Mok GSP. Evaluation of sequential SPECT and CT for targeted radionuclide therapy dosimetry. Ann Nucl Med. 2018;32:34-43.
5. Li T, Mok GSP. Technical Note: Virtual CT for reducing CT dose in targeted radionuclide therapy dosimetry. Med Phys. 2018;45:5138-44.
6. Schillaci O, Spanu A, Tagliabue L, Filippi L, Danieli R, Palumbo B, et al. SPECT/CT with a hybrid imaging system in the study of lower gastrointestinal bleeding with technetium-99m red blood cells. Q J Nucl Med Mol Imaging. 2009;53:281-9.
7. Zhang D, Yang B-H, Wu NY, Mok GSP. Respiratory average CT for attenuation correction in myocardial perfusion SPECT/CT. Ann Nucl Med. 2017;31:172-80.
8. Nakamoto Y, Tatsumi M, Cohade C, Osman M, Marshall LT, Wahl RL. Accuracy of image fusion of normal upper abdominal organs visualized with PET/CT. Eur J Nucl Med Mol Imaging. 2003;30:597-602.
9. Sun T, Mok GS. Techniques for respiration-induced artifacts reductions in thoracic PET/CT. Quant Imaging Med Surg. 2012;2:46-52. https://doi.org/10.3978/j.issn.2223-4292.2012.02.01.
10. Ho CY, Wu T-H, Mok GSJNmc. Interpolated average CT for PET attenuation correction in different lesion characteristics. Nucl Med Commun. 2016;37:297-306.
11. Mok GS, Ho CY, Yang B-H, Wu T-HJJoNC. Interpolated average CT for cardiac PET/CT attenuation correction. J Nucl Cardiol. 2016;23:1072-9.
12. Sun T, Wu TH, Wang SJ, Yang BH, Wu NY, Mok GS. Low dose interpolated average CT for thoracic PET/CT attenuation correction using an active breathing controller. Med Phys. 2013;40:102507.
13. He B, Frey EC. The impact of 3D volume of interest definition on accuracy and precision of activity estimation in quantitative SPECT and planar processing methods. Phys Med Biol. 2010;55:3535-44. https://doi.org/10.1088/0031-9155/55/12/017.
14. Goetze S, Brown TL, Lavely WC, Zhang Z, Bengel FM. Attenuation correction in myocardial perfusion SPECT/CT: effects of misregistration and value of reregistration. J Nucl Med. 2007;48:1090-5. https://doi.org/10.2967/jnumed.107.040535.
15. Sjögreen-Gleisner K, Rueckert D, Ljungberg M. Registration of serial SPECT/CT images for three-dimensional dosimetry in radionuclide therapy. Phys Med Biol. 2009;54:6181-200.
16. Segars WP, Sturgeon G, Mendonca S, Grimes J, Tsui BM. 4D XCAT phantom for multimodality imaging research. Med Phys. 2010;37:4902-15. https://doi.org/10.1118/1.3480985.

17. He B, Du Y, Segars WP, Wahl RL, Sgouros G, Jacene H, et al. Evaluation of quantitative imaging methods for organ activity and residence time estimation using a population of phantoms having realistic variations in anatomy and uptake. Med Phys. 2009;36:612-9. https://doi.org/10.1118/1.3063156.

18. Frey E, Tsui B. A practical projector-backprojector modeling attenuation, detector response, and scatter for accurate scatter compensation in SPECT. Conference Record of the 1991 IEEE Nuclear Science Symposium and Medical Imaging Conference. 1991;3:1777-81.

19. Seo Y, Wong KH, Hasegawa BH. Calculation and validation of the use of effective attenuation coefficient for attenuation correction in In‐111 SPECT. Med Phys. 2005;32:3628-35.

20. Frey EC, Tsui B. A new method for modeling the spatially-variant, object-dependent scatter response function in SPECT. 1996 IEEE Nuclear Science Symposium Conference Record. 1996;2:1082-6.

21. Metz CE, Atkins F, Beck RN. The geometric transfer function component for scintillation camera collimators with straight parallel holes. Phys Med Biol. 1980;25:1059-70.

22. Yushkevich PA, Piven J, Hazlett HC, Smith RG, Ho S, Gee JC, et al. User-guided 3D active contour segmentation of anatomical structures: significantly improved efficiency and reliability. Neuroimage. 2006;31:1116-28. https://doi.org/10.1016/j.neuroimage.2006.01.015.

23. Song N, He B, Frey E. The effect of volume-of-interest misregistration on quantitative planar activity and dose estimation. Phys Med Biol. 2010;55:5483-97. https://doi.org/10.1088/0031-9155/55/18/014.

24. Ao EC, Wu NY, Wang SJ, Song N, Mok GS. Improved dosimetry for targeted radionuclide therapy using nonrigid registration on sequential SPECT images. Med Phys. 2015;42:1060-70.

25. Klein S, Staring M, Murphy K, Viergever MA, Pluim JP. Elastix: a toolbox for intensity-based medical image registration. IEEE Trans Med Imaging. 2009;29:196-205.

26. Lu Z, Chen G, Lin KH, Wu TH, Mok GS. Evaluation of Different CT Maps for Attenuation Correction and Segmentation in Static 99mTc‐MAA SPECT/CT for 90Y Radioembolization Treatment Planning – a Simulation Study. Med Phys. 2021.

27. Bastiaannet R, Viergever MA, de Jong HW. Impact of respiratory motion and acquisition settings on SPECT liver dosimetry for radioembolization. Med Phys. 2017;44:5270-9.

28. He B, Du Y, Song X, Segars WP, Frey EC. A Monte Carlo and physical phantom evaluation of quantitative In-111 SPECT. Phys Med Biol. 2005;50:4169-85.